3-D Assessment of Neutron Streaming through Inboard Assembly Gaps of ARIES Tokamak Power Plant

T.D. Bohm, L.A. El-Guebaly and the ARIES Team

June 2009

UWFDM-1364

FUSION TECHNOLOGY INSTITUTE

UNIVERSITY OF WISCONSIN

MADISON WISCONSIN

3-D Assessment of Neutron Streaming through Inboard Assembly Gaps of ARIES Tokamak Power Plant

T.D. Bohm, L.A. El-Guebaly and the ARIES Team
tdbohm@wisc.edu

Fusion Technology Institute
University of Wisconsin
1500 Engineering Drive
Madison, WI 53706

http://fti.neep.wisc.edu

June 2009

UWFDM-1364

1. Introduction

In the ARIES-AT tokamak design[1], blanket modules are arranged around the plasma to provide thermal and nuclear shielding for the vacuum vessel and magnets and to provide tritium breeding capability for the power plant. The in-vessel components are segmented in the toroidal direction and there are 16 modules in the inboard (IB) and outboard (OB) sides.

There are gaps between adjacent blanket and shield modules to allow for thermal expansion, neutron induced swelling, and to allow for radial removal by remote handling equipment. These gaps allow increased levels of neutron and gamma radiation to reach components behind the modules. These increased levels could possibly exceed radiation damage or heating limits for some components. Radiation streaming through these gaps needs to be assessed and any problems identified need to be solved by design. Substantial earlier work has been done in analyzing the effect of gaps between modules on nuclear parameters.[2-7]

From the assembly and disassembly viewpoint, a straight gap is the simplest, most favorable option. However, to attenuate the streaming radiation efficiently, a stepped gap is highly desirable. Earlier work has shown that each 90^{o} bend could potentially reduce the damage by 5-fold. As such, a proposed design to solve the ARIES streaming issue included double stepping the gap. To further attenuate the streaming neutrons, El-Guebaly suggested inserting a WC (or W) shield block within the double step area. This novel idea seems to provide additional shielding benefits, as will be discussed later. The block was carefully configured to allow a maintainable geometry. Based on past shielding analysis, WC offers better shielding performance than W.

In this work, streaming through both straight and stepped poloidal gaps was analyzed for the IB components of the preliminary dual coolant lithium lead (DCLL) blanket design for ARIES-AT. In particular, the effect of these gaps on radiation damage parameters for the winding pack, vacuum vessel, manifolds, shield and first wall were determined. The MCNPX v2.7.A three dimensional (3-D) Monte Carlo transport code[8] and FENDL-2.1 cross section library[9] were used.

2. Model

In this work, the basis for the examined design is the ARIES-AT DCLL radial build as defined by El-Guebaly.[10] Figure 1 shows the IB radial build with the LiPb/He manifolds option. The design was implemented in the MCNPX geometry using CAD drawings of various components when available. Not all of the details present in the CAD drawings were implemented; instead, a partially homogenized model was created since the current design is still evolving.

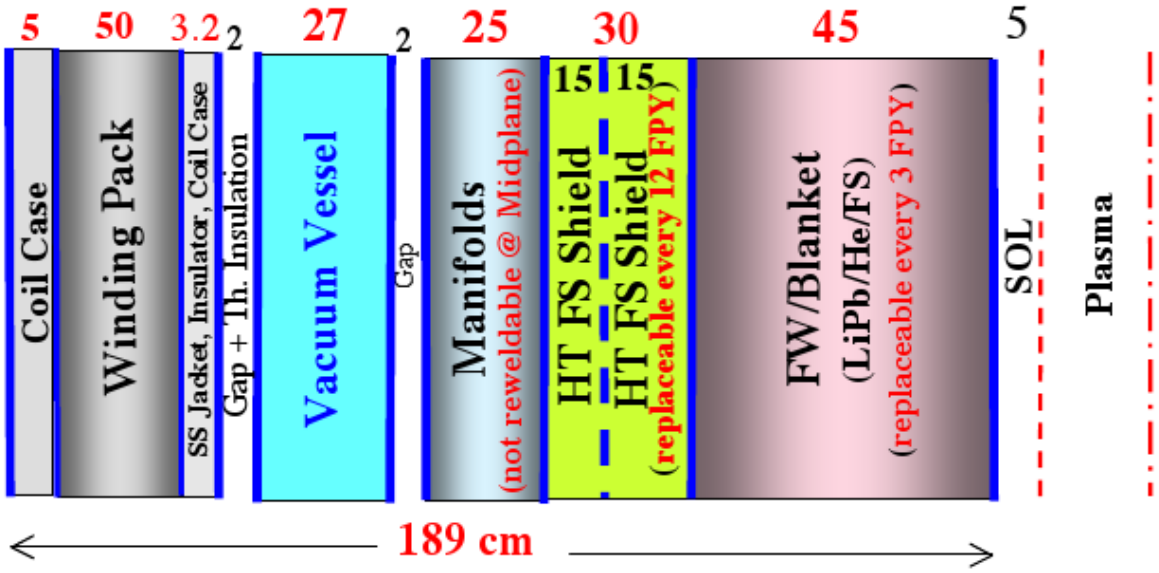

Figure 1. Schematic of IB radial build for the ARIES-AT DCLL design.[10]

Figure 2 shows a slice through the 3-D model used in MCNPX to model the design. This is an 11.25° sector representing half of a module with the reflecting boundaries indicated. The vertical extent of the model is 100 cm with reflecting boundaries on the top and bottom. Shown in Figure 2 is the IB first wall (FW), blanket (BL), shield (SH), manifolds, vacuum vessel (VV), and magnet. The magnet includes the case and winding pack (WP). On the OB side, only the FW and blanket are modeled since this is sufficient to provide adequate radiation reflection conditions without modeling the entire OB side. The OB FW is 3.8 cm thick with the same composition as the IB FW. The OB blanket is 70 cm thick with the same composition as the IB blanket.

A uniform volumetric 14.1 MeV neutron source in the outer region of the plasma volume (r=460-625 cm) is used as shown in Figure 2. All calculations are normalized for a neutron wall loading of 3.4 MW/m^2 which is the peak value at the IB midplane.

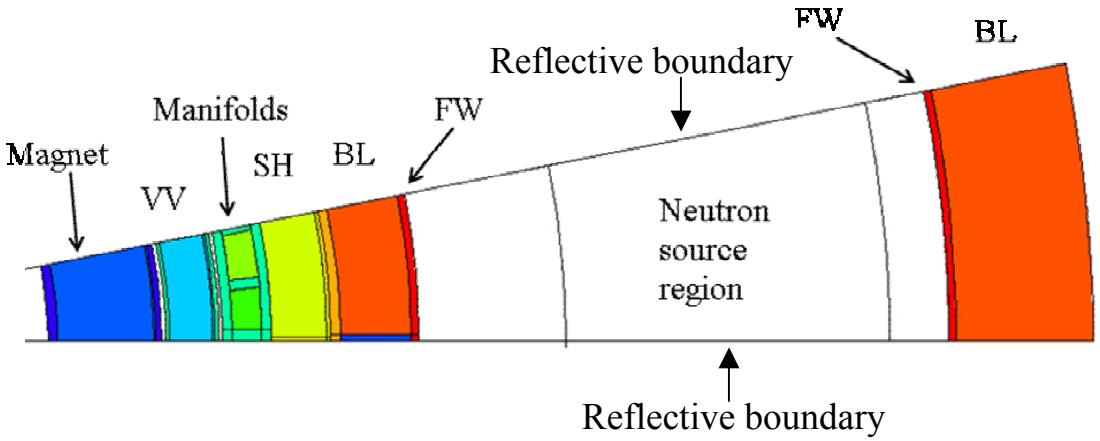

Figure 2. Slice through MCNPX model created for ARIES-AT DCLL design.

2a. No gap case

Figure 3 shows the MCNPX model for the "no gap" case examined in this work. This model includes two significant details from the ARIES-AT DCLL design. First, the He and LiPb manifolds between the SH and VV components are included. Figure 4 shows a CAD drawing of the He and LiPb manifolds for the OB side of the ARIES-AT DCLL design. The IB design has 4 manifolds with He manifolds on the outside of the module and LiPb manifolds in the interior. Second, the model includes sidewalls along the module edges.

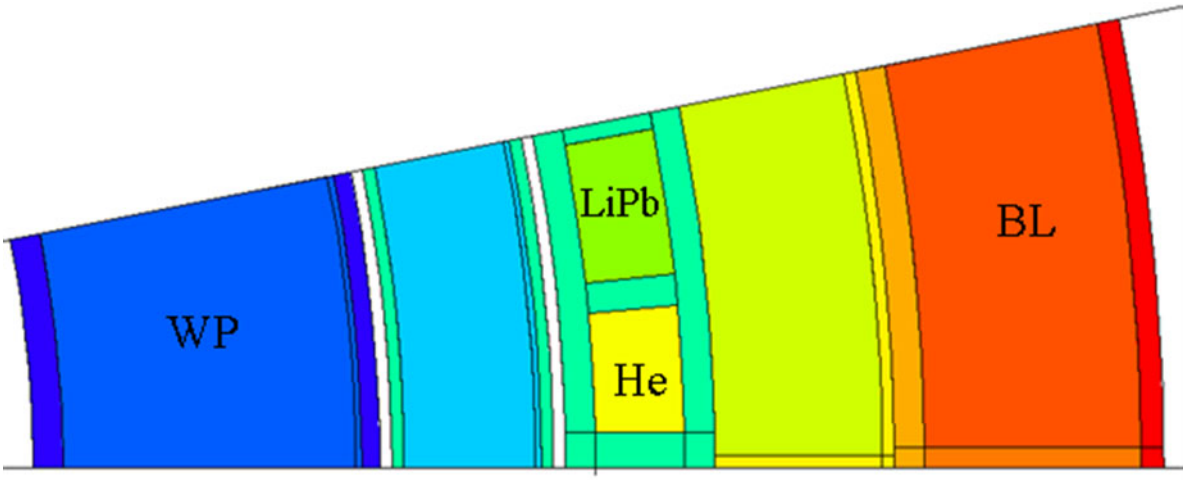

Figure 3. No gap MCNPX model showing LiPb manifold, He manifold, and sidewalls.

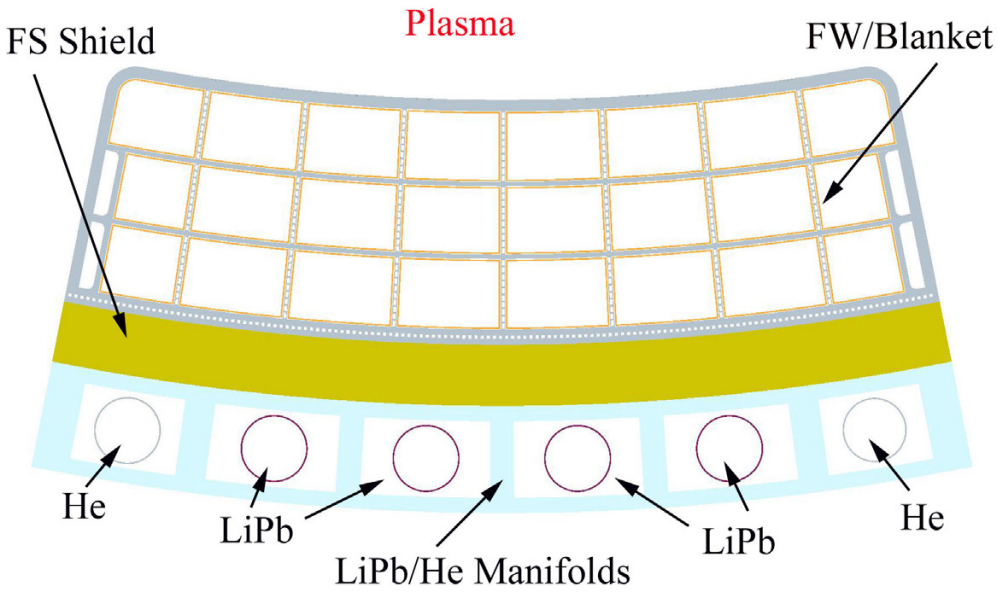

Figure 4. CAD drawing of OB module showing detail of manifolds.

2b. Straight gap case

For this work, 1 cm and 2 cm wide straight gaps were investigated. Figure 5 shows the CAD drawing for the straight gap design while Figure 6 shows the MCNPX straight gap model. Note that the gap penetrates all the way to the VV. Also, because of the reflecting boundary condition along the bottom edge of the wedge, the gap is modeled as half the gap width.

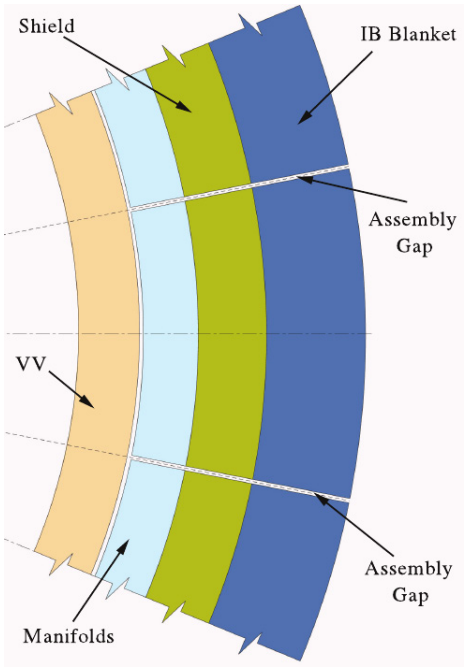

Figure 5. CAD drawing of straight gap design.

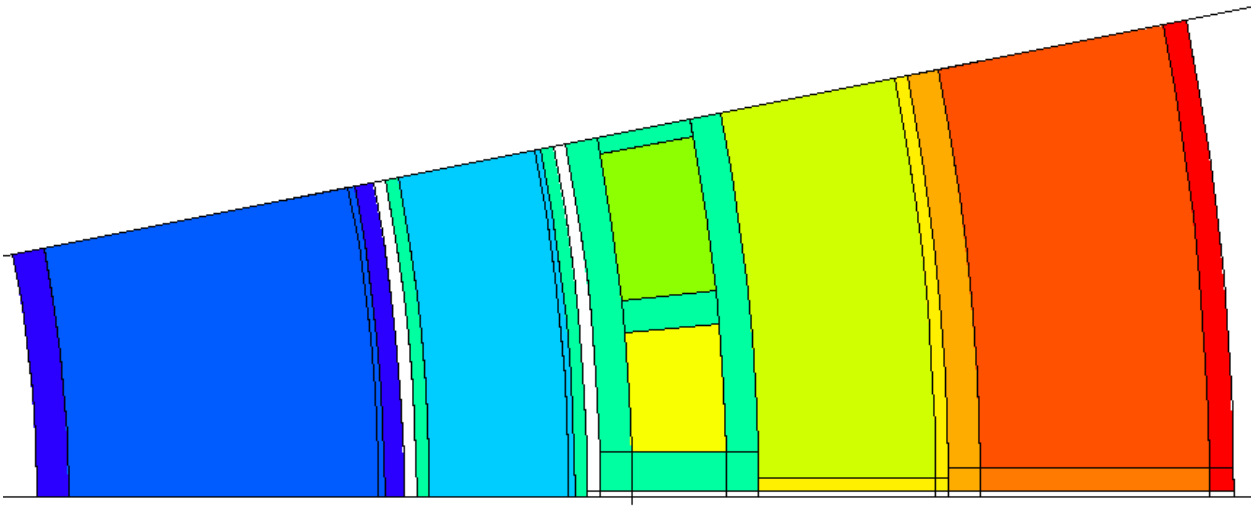

Figure 6. Straight gap MCNPX model.

2c. Stepped gap case

Figure 7 shows the CAD drawing for the stepped gap design while Figure 8 shows the MCNPX stepped gap model. Note that the stepped gap design includes 2 steps with 5 cm offsets and a shield block filling the gap space. Figure 9 shows the definition of the offset. For this work, 1 and 2 cm wide gaps were investigated with a WC shield block.

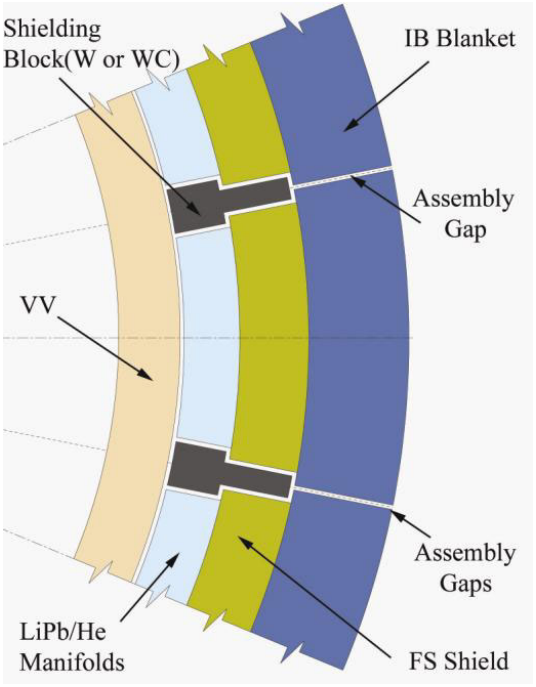

Figure 7. CAD drawing of stepped gap design.

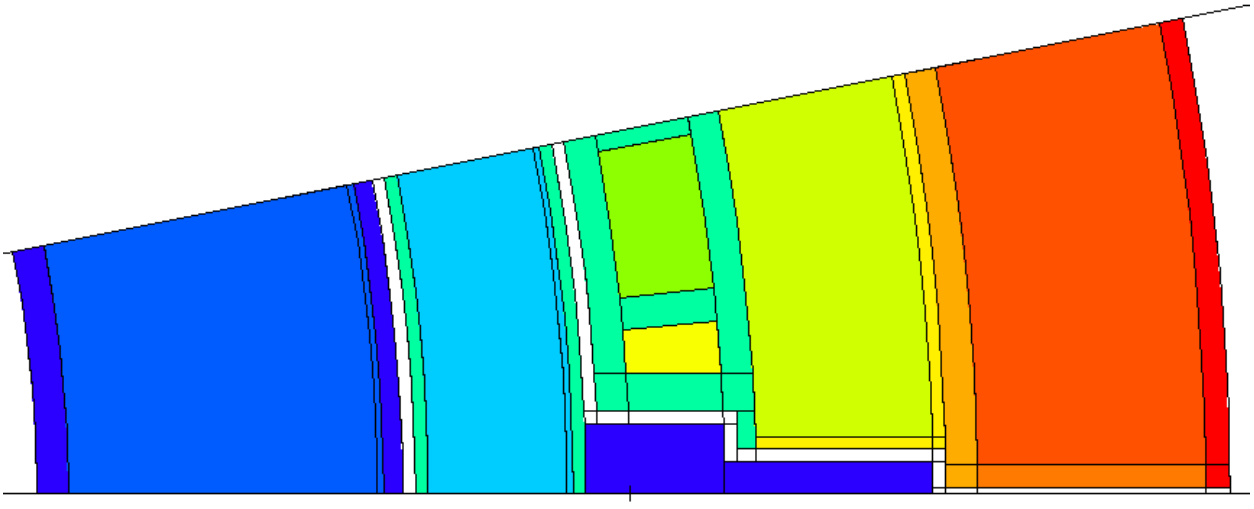

Figure 8. Stepped gap MCNPX model.

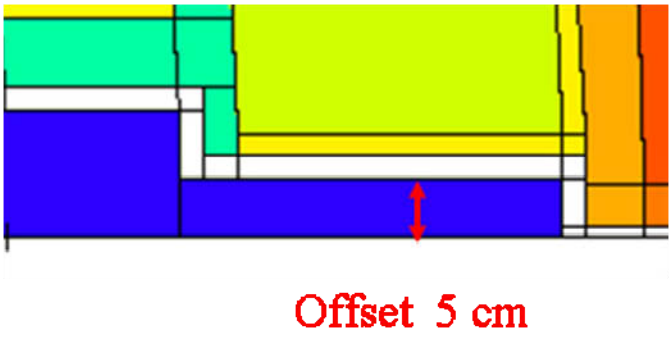

Figure 9. Close up view of the MCNPX model showing the definition of the stepped gap offset.

3. Results

In order to illustrate the nuclear environment on the IB side of the ARIES-AT DCLL design, the fast neutron (E>0.1 MeV) flux was calculated at the front surfaces of various components in the no gap model. Figure 10 shows the fast neutron flux as a function of the angle theta at the front surface of various components in the model. Figure 11 shows the radial location of the graph profiles and the definition of the angle theta. Figure 10 shows that there is almost 6 orders of magnitude of fast neutron flux attenuation from the FW to the WP. Also note the higher flux levels at angles of 0-5^{o} for the VV and WP. For example, the WP flux at 0^{o} is about 2 times the flux at 11^{o}. This is because the He manifold does not provide as much neutron attenuation as the LiPb manifold.

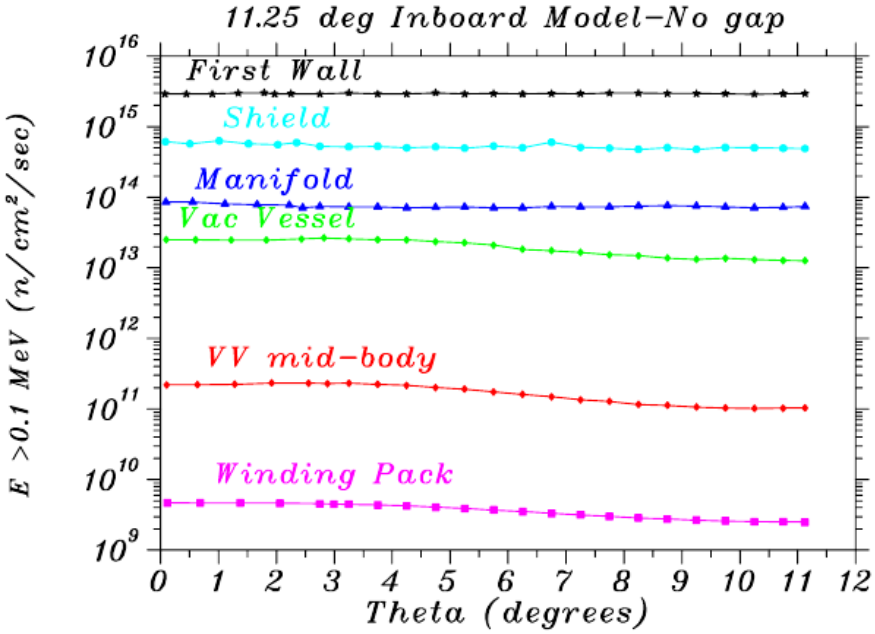

Figure 10. Fast neutron flux at the surface of various components as a function of the angle theta for the no gap model.

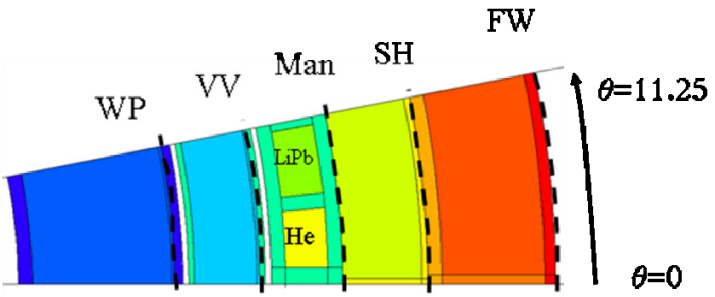

Figure 11. No gap model showing the location of fast neutron flux profiles plotted in Figure 10 and the definition of the angle theta.

3a. dpa at Shield Front

Figure 12 shows the dpa after 40 full power years (FPY) in ferritic steel (FS) at the front of the IB shield as a function o f the angle theta for the no gap, 2 cm straight gap and 2 cm stepped gap cases. Figure 13 shows the corresponding graphs for 1 cm gaps. Figure 14 shows the location of the graph profiles and the definition of the angle theta for the stepped gap. Because of the gap, the shield does not exist in the region near theta=0 (see Figure 14). Therefore, the location of the start of the shield is indicated on Figures 12 and 13 as well as the corresponding value for dpa. Additionally, a dotted line indicating the dpa limit (200 dpa/40 FPY) is shown for reference.

There are several notable features shown in Figure 12 and 13. First, looking at the no gap case, the dpa is higher at angles near 0 degrees. This is because the blanket sidewalls have reduced shielding effectiveness as compared to the body of the blanket. Next, both the straight and stepped gap cases show substantial peaking. The gap/nogap ratios are as high as 1.3 for the 2 cm straight gap and 1.1 for the 2 cm stepped gap. Note that the shape of the curves are similar for the straight and stepped gap cases since at this depth, the stepped gap has not begun its stepping portion and still looks like a straight gap for the shield (this can be seen in Figure 14). Further note that as one moves away from the gap (0-1 degrees) toward higher values of the angle theta, there is not an abrupt decrease in the dpa, but instead a gradual decline in the radiation damage. Finally, all cases exceed the dpa limit so this indicates that the front part of the shield must be replaceable.

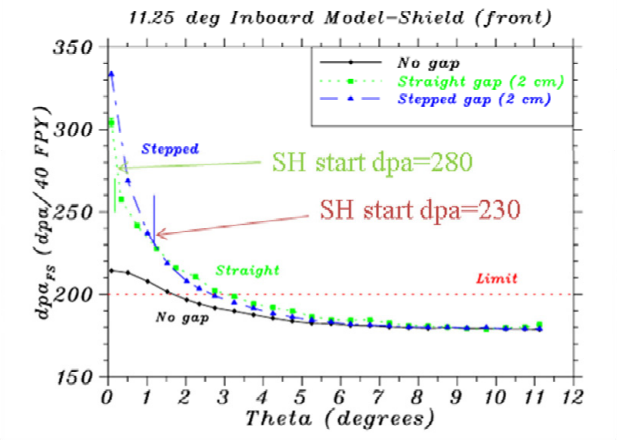

Figure 12. dpa at shield front for 2 cm gaps.

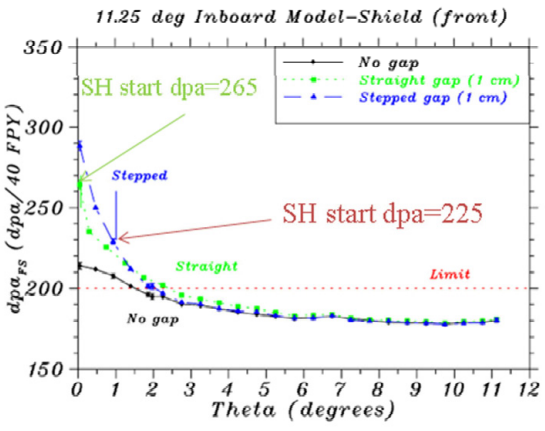

Figure 13. dpa at shield front for 1 cm gaps.

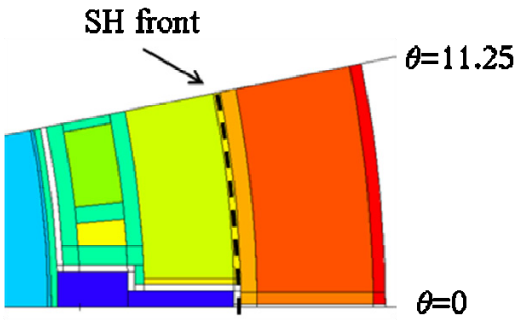

Figure 14. Stepped gap model showing the location of dpa profiles shown in Figure 12 and Figure 13 and the definition of the angle theta.

3b. He Production at Manifold Front

Figure 15 shows the He production after 40 FPY in FS at the front of the IB manifolds as a function of the angle theta for the no gap, 2 cm straight gap and 2 cm stepped gap cases. Figure 16 shows the corresponding graphs for 1 cm gaps. Figure 17 shows the location of the graph profiles and the definition of the angle theta for the stepped gap. Because of the gap, and in the case of the stepped gap, the WC shield block, the manifold does not exist in the region near theta=0 (see Figure 17). Therefore, the location of the start of the manifold is indicated on Figures 15 and 16 and the corresponding value for He production. Additionally, a dotted line indicating the He production limit for reweldability of ferritic steel (FS) (1 appm/40 FPY) is shown for reference.

Looking at Figures 15 and 16, there are several key features to observe. First, the peaking in the gap/no gap ratios is large, as much as 30 for the straight 2 cm gap and 8 for the stepped 2 cm gap. Also, for the stepped gap cases, the peak is shifted due to the first step. Finally, in all cases, the He production limit is exceeded so the front part of the manifold is not reweldable.

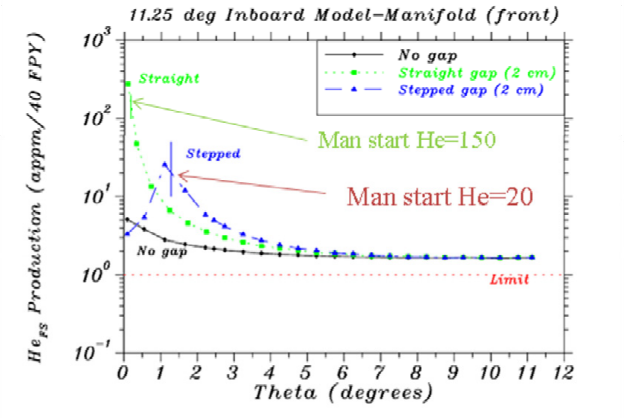

Figure 15. He production at manifold front for 2 cm gaps.

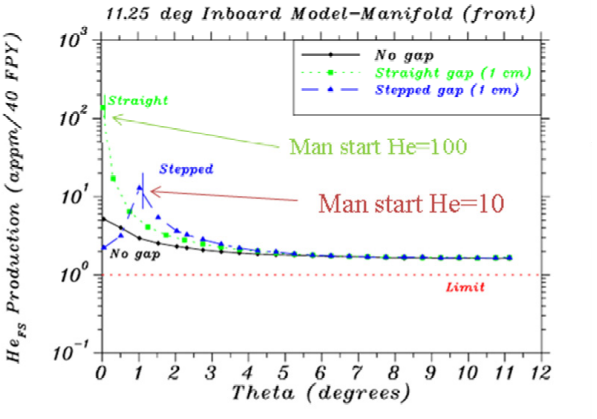

Figure 16. He production at manifold front for 1 cm gaps.

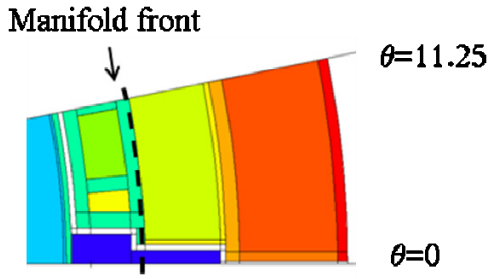

Figure 17. Stepped gap model showing the location of He production profiles plotted in Figure 15 and Figure 16 and the definition of the angle theta.

3c. He Production at Vacuum Vessel Front

Figure 18 shows the He production after 40 FPY in FS at the front of the VV as a function of the angle theta for the no gap, 2 cm straight gap and 2 cm stepped gap cases. Figure 19 shows the corresponding graphs for 1 cm gaps. Figure 20 shows the location of the graph profiles and the definition of the angle theta for the stepped gap. Notice that the VV spans the whole 11.25 degree model.

Looking at Figures 18 and 19, shows the straight gap leads to very strong peaking, the gap to no gap ratio is as high as 900 for a 2 cm gap. The stepped gap is much less peaked with a gap to no gap ratio of up to 1.7 for a 2 cm stepped gap. Notice also that the peak in the stepped gap cases is shifted to higher values of theta (2.5 degrees) compared to the peaks for the manifold (1 degree). This is because the VV sees the effect of the double step. Finally, notice that the no gap and stepped gap cases meet the He production limit of 1 appm for reweldability of FS.

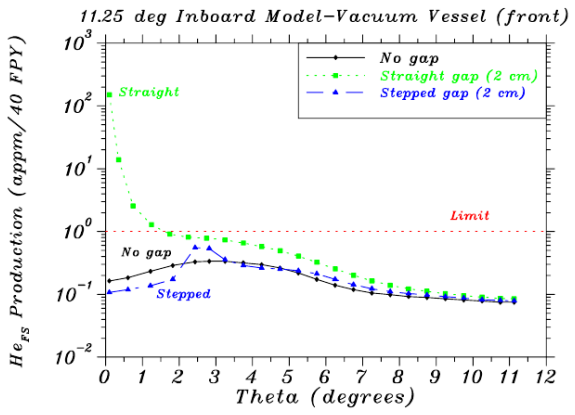

Figure 18. He production at VV front for 2 cm gaps.

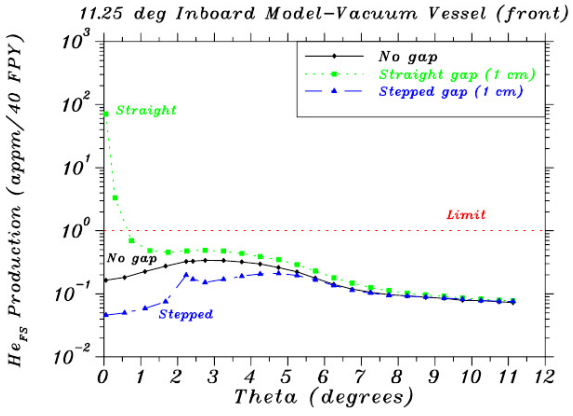

Figure 19. He production at VV front for 1 cm gaps.

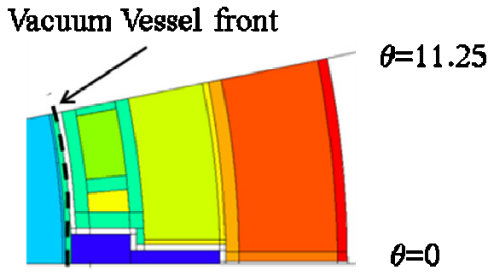

Figure 20. Stepped gap model showing the location of He production profiles plotted in Figure 18 and Figure 19 and the definition of the angle theta.

3d. Fast Fluence at Winding Pack Front

Figure 21 shows the fast neutron fluence (E>0.1 MeV) after 40 FPY at the front of the WP as a function of the angle theta for the no gap, 2 cm straight gap and 2 cm stepped gap cases. Figure 22 shows the corresponding graphs for 1 cm gaps. Figure 23 shows the location of the graph profiles and the definition of the angle theta for the stepped gap. Notice that the WP spans the whole 11.25 degree model.

Looking at Figures 21 and 22 clearly shows smoother peaking than seen at the front of the VV, manifolds, or shield. This is because the gap does not penetrate through the VV and the VV provides some shielding near the gap locations (see Figure 23). The straight gap still shows significant peaking in the gap to no gap ratio, up to 9.5 for 2 cm gaps. Additionally, notice for the stepped gap case that the fluence is reduced compared to the no gap case even for angles away from the gap and WC shield block. Finally, the stepped gap meets the fast neutron fluence limit of 1e19 n/cm^2 at 40 FPY for the winding pack.

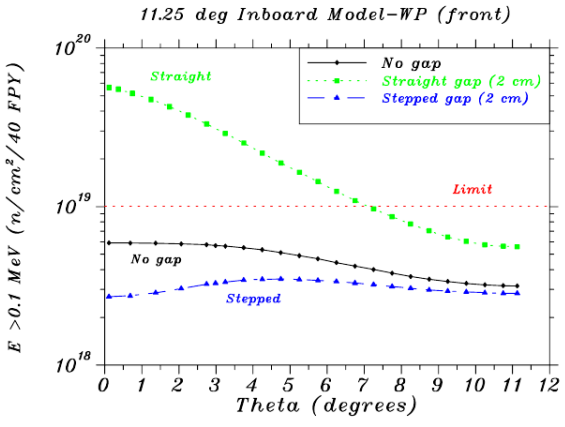

Figure 21. Fast neutron fluence at WP front for 2 cm gaps.

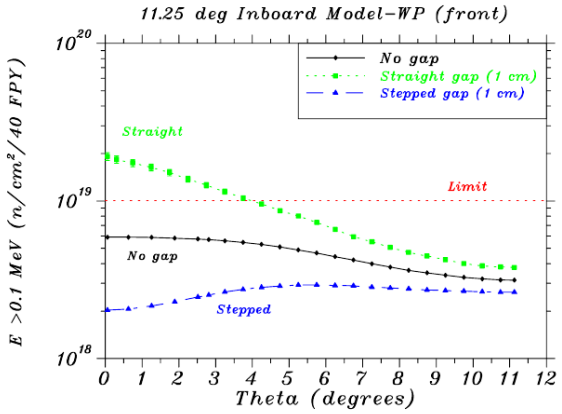

Figure 22. Fast neutron fluence at WP front for 1 cm gaps.

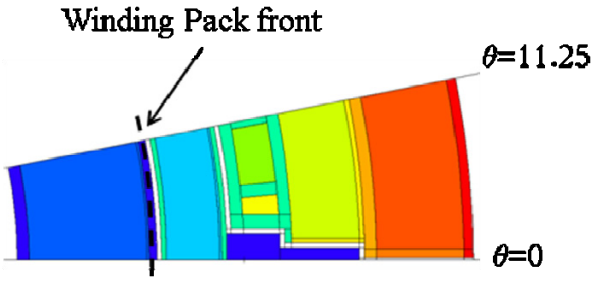

Figure 23. Stepped gap model showing the location of fast neutron fluence profiles shown in Figure 21 and Figure 22 and the definition of the angle theta.

3e. Heating in WC Shield Block

An important consideration for the WC shield block used in the stepped gap design is the level of nuclear heating. A preliminary calculation by Malang[11] has shown that radiative cooling is feasible if the average heating in the block is below 15 W/cm^3 and if a block temperature >1000^{o}C is allowed.

Figure 24 shows the nuclear heating in W/cm^3 in the WC shield block for a 2 cm stepped gap. For reference, Figure 25 shows the location of the shield block in the stepped gap model. The peak heating (16.7 W/cm^3) is indicated in Figure 24 and is nearest the plasma and gap as expected. The average heating in the section of the block close to the plasma (x=305-338 cm) is 6.2 W/cm^3. The average heating in the section furthest from the plasma (x=283-305 cm) is 1.0 W/cm^3. The average nuclear heating in the whole block is 3.1 W/cm^3. The poloidal average heating is even lower considering the 1.3 reduction in the average IB NWL compared to the peak NWL value at the midplane. Since this is well below 15 W/cm^3, this indicates that radiative cooling of the WC shield block is feasible.

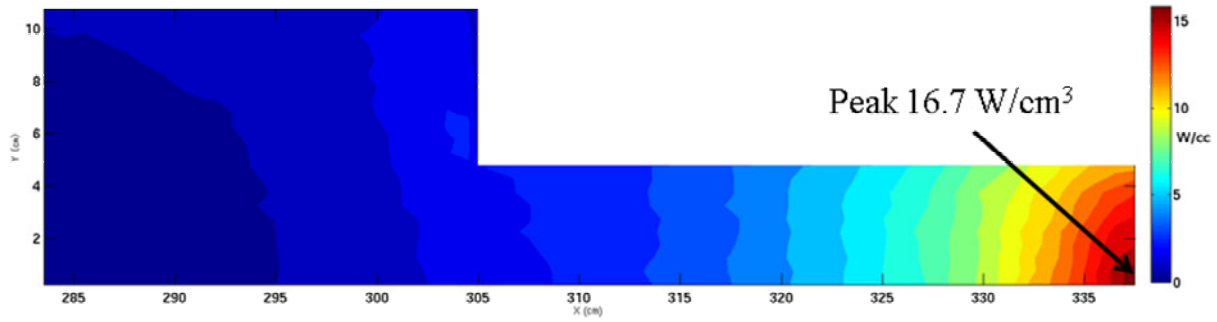

Figure 24. Nuclear heating (W/cm^3) in the WC shield block used in the stepped gap design.

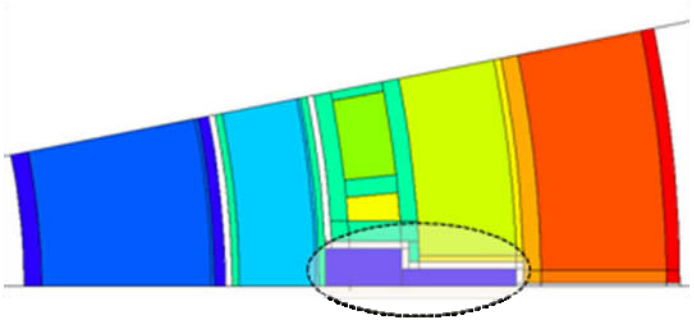

Figure 25. Location of WC shield block in the stepped gap model.

3f. dpa in WC Shield Block

The dpa in the WC shield block is an important parameter to material scientists to determine if the WC shield block can be used as a structural component. Figure 26 shows the carbon dpa and tungsten dpa in the shield block as a function of radial position along the theta=0 angle. The location of these graph profiles is indicated in Figure 27 and 28. The carbon dpa peaks at 17 dpa/FPY and the tungsten dpa peaks at 2.6 dpa/FPY. At this time, the dpa limit for structural use of WC is not known so we cannot make any conclusions as to the suitability of WC for structural material in this design. More work will need to be done in the material science field for assessing radiation damage in WC.

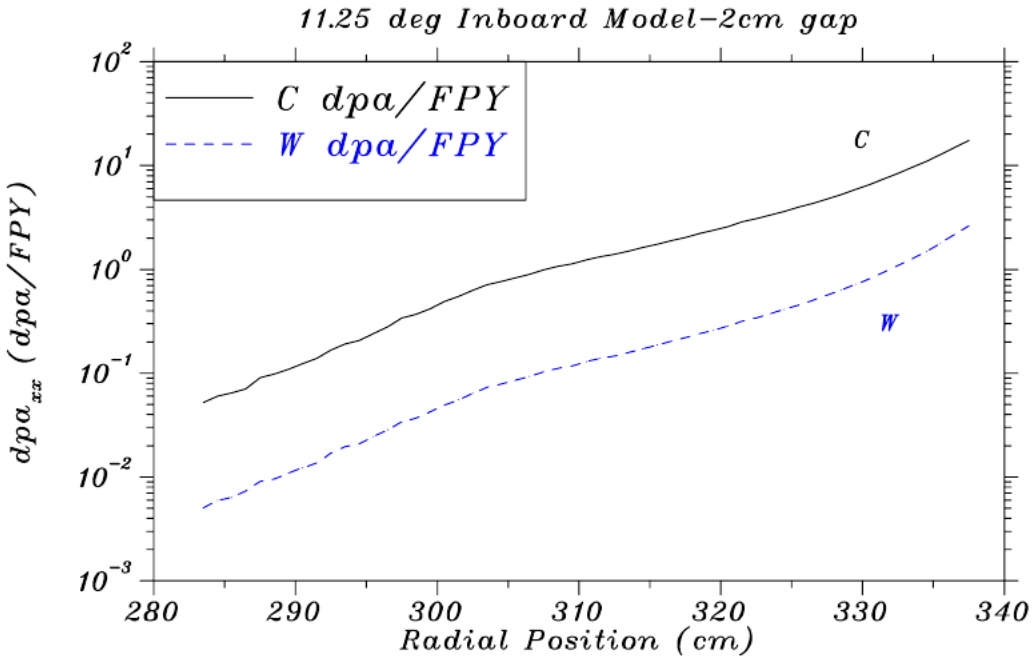

Figure 26. dpa in WC shield block along the theta=0 position.

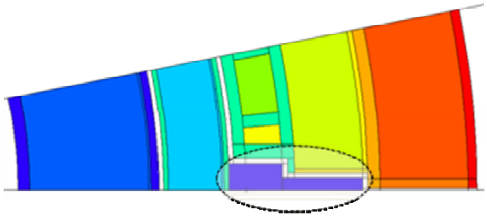

Figure 27. Location of WC shield block.

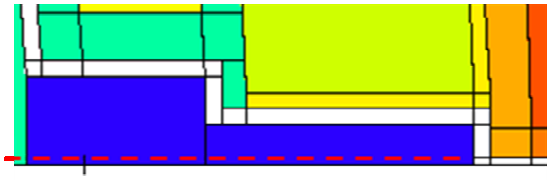

Figure 28. Location of C and W dpa profiles plotted in Figure 26.

4. Conclusions

In this work, straight and stepped 1 cm and 2 cm wide poloidal gaps were examined for a particular ARIES-AT DCLL design. It was found that straight gaps allow too much radiation to reach components on the IB side of the tokamak. This streaming problem was solved with a double stepped gap and WC shield block. The double stepped gap and WC shield block were effective at protecting the IB VV and magnet.

This work did not include a safety factor to account for nuclear data uncertainty and will have to be addressed in future work. Following this uncertainty assessment, a safety factor can be determined for use with 1-D models which includes the combined effect of the gap and nuclear data uncertainty.

Acknowledgments

This work was performed under the auspices of the U.S. Department of Energy (contract #DE-FG02-98ER 54462). The authors would like to thank our colleagues on the ARIES team for providing useful inputs and comments: S. Malang (Germany), L. Waganer (Boeing), R. Raffray and X. Wang (UCSD).

REFERENCES

1. L.A. EL-GUEBALY, "Nuclear Performance Assessment of ARIES-AT," *Fusion Engineering and Design*, 80, 99-110 (2006).

2. T.D. BOHM, M.E. SAWAN, P. WILSON, "Radiation Streaming in Gaps between ITER First Wall Shield Modules", *Fusion Science and Technology*, in press (2009).

3. H. IIDA, L. PETRIZZI, V. KHRIPUNOV, G. FEDERICI, and E. POLUNOVSKIY, "Nuclear Analyses of Some Key Aspects of the ITER Design with Monte Carlo Codes", *Fusion Engineering and Design*, **74**, 133-139 (2005).

4. H. IIDA, V. KHRIPUNOV, L. PETRIZZI, G. FEDERICI , "Nuclear Analysis Report", ITER Design Description Document, G 73 DDD 2 W 0.2, July (2004).

5. L.A. EL-GUEBALY and M.E. SAWAN, "Shielding Analysis for ITER with Impact of Assembly Gaps and Design Inhomogeneities", Proc. 8th International Conf. on Radiation Shielding, Arlington, Texas, 24-28 April 1994, 1047-1054 (1994).

6. S. SATO, H. IIDA, R. PLENTEDA, R. SANTORO, "Monte Carlo Analysis of Helium Production in the ITER Shielding Blanket Module", *Fusion Engineering and Design*, **46**, 1-9, October (1999).

7. S. SATO, Y. SEKI, H. TAKATSU, T. UTSUMI, "Streaming Analysis of Gap Between Blanket Modules for Fusion Experimental Reactor", *Fusion Technology*, **30/3**, 1129-1133, December (1996).

8. D. PELOWITZ et al., "MCNPX 2.7.A Extensions", Los Alamos National Laboratory Report, LA-UR-08-07182, November 6 (2008).

9. D.L. ALDAMA and A. TRKOV, "FENDL-2.1, Update of an Evaluated Nuclear Data Library for Fusion Applications," Report INDC(NDS)-467, International Atomic Energy Agency (2004).

10. L.A. EL-GUEBALY, "ARIES-AT Radial Build Definition: DCLL Blanket with Thin SiC Inserts", presented at ARIES Pathways Project meeting, January 21-22, 2009.

11. S. MALANG (Germany), private communication, 2/25/2009.